Heliyon 10 (2024) e33282

Contents lists available at ScienceDirect

Heliyon

journal homepage: www.cell.com/heliyon

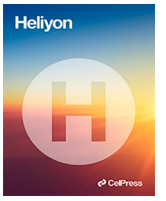

Research article

Influence of fullerene content on the properties of polyurethane resins: A study of rheology and thermal characteristics

Nazym Ye Akhanova [a,b], El-Sayed Negim [a,c], Yerassyl Yerlanuly [a,b,d], Didar G. Batryshev [a], Mohamed M. Eissa [e], Dmitry Yu Schur [f], Tlekkabul S. Ramazanov [b,d], Khaldun M. Al Azzam [g], Mukhit M. Muratov [b,d], Maratbek T. Gabdullin [a,*]

[a] Kazakh-British Technical University, 59 Tole Bi St., 050000, Almaty, Kazakhstan
[b] National Nanotechnological Laboratory of Open Type (NNLOT), Al-Faraby Kazakh National University, 71, Al-Faraby Ave., 050040, Almaty, Kazakhstan
[c] School of Petroleum Engineering, Satbayev University, 22 Satpayev Street, 050013, Almaty, Kazakhstan
[d] Kazakh Physical Society, 050040, Republic of Kazakhstan, Almaty, Al-Farabi Ave. 71, Kazakhstan
[e] Polymers and Pigments Department, National Research Centre, 33 El Bohouth St., Dokki, Giza, 12622, Egypt
[f] Institute for Problems of Materials Science National Academy of Sciences in Ukraine, UA-03142, Kyiv, Ukraine
[g] Department of Chemistry, Faculty of Science, The University of Jordan, 11942, Amman, Jordan

ARTICLE INFO

Keywords:
Polyurethane
Fullerene
Isocyanate
Rheology
Thermal properties

ABSTRACT

The effect of different contents of fullerene on the properties of polyurethane resins (PUs), including rheology and thermal properties, was investigated. Polyurethane resins were prepared through polyaddition reactions using different isocyanate monomers such as isophorone diisocyanate (IPDI), methylene diphenyl diisocyanate (MDI), hexamethylene diisocyanate (HDI), and different polyols, such as poly(oxytetramethylene) glycol (PTMG), the triol trade name FA-703, and polypropylene glycols (PPG), at an NCO/OH ratio 0.94 and a temperature of 100 °C. IR spectroscopy was used to control the polymerization of PUs through the shifting of NCO peaks. The results showed that the rheology and thermal properties of the prepared PU resins depend on the type of isocyanates and fullerene used. Based on the type of isocyanates, the PU resin prepared by MDI has the highest viscosity and thermal stability compared to the other isocyanates investigated. On the other hand, the PU resins prepared by IPDI mixed with fullerene had the highest viscosity and thermal stability. However, the initial decomposition temperature (*T* onset) of the PUs decreased with the addition of fullerene without affecting the maximum decomposition temperature (PDT_{max}) of the PU resin.

1. Introduction

In its sp^2 hybridized state, elemental carbon can give rise to fascinating structures known as allotropes. These allotropes have a wide range of industrial applications, including diamond, graphite, graphene, carbon nanotubes, and fullerenes. Fullerenes, which are part of this diverse carbon-only molecule family, exhibit distinctive hollow spheres, ellipsoids, or tube structures resembling soccer

* Corresponding author.
E-mail address: gabdullin.kbtu@gmail.com (M.T. Gabdullin).

https://doi.org/10.1016/j.heliyon.2024.e33282
Received 23 February 2024; Received in revised form 14 June 2024; Accepted 18 June 2024
Available online 20 June 2024

balls [1]. Fullerenes typically follow the general formula Cn, where n is greater than 20, with C_{60} and C_{70} being the most common variants. Their exceptional physical, chemical, electrical, and optical properties make them valuable components in the development of new and enhanced devices and materials, leading to their extensive use in the fields of science, engineering, and industry [2]. Fullerene is a polycyclic aromatic hydrocarbon and a stable organic compound composed of more than two aromatic rings. Fullerene can be soluble in different solvents and has different photophysical characteristics than other polyaromatic compounds [3–11]. The use of fullerene in optical, organic light-emitting, biomedical, and coating applications has been investigated [12–17].

Composites are a new class of materials prepared by incorporating fullerene into the molecular chains of different kinds of polymers, including acrylic, epoxy, and polyurethanes, to increase outstanding properties such as thermal stability, chemical resistance, mechanical properties and corrosion protection [18–21]. Previously, fullerenes were used as additives in polyester urethane to reduce the hydrogen permeability of stainless steel [22]. Considering this factor, research on various polymers with the addition of fullerenes and the study of their properties are relevant tasks.

Additionally, Kanbur et al. (2018) [23] studied the mechanical, thermal, and flame resistance characteristics of fullerene-loaded thermoplastic polyurethane composites. They developed multifunctional polyurethane elastomer composites incorporating fullerene, which exhibit mechanical, damping, thermal, and flammability properties. According to their findings, adding C_{60} to thermoplastic polyurethane resulted in a nearly twofold increase in the tensile strength, % elongation, and Young's modulus. The shore hardness of thermoplastic polyurethane decreases with the addition of C_{60}. Dobashi et al. (2013) [24] used fullerene as a filler because it is soluble in various organic solvents and is very straightforward to chemically modify. Adding urethanized fullerene, a chemical modification of fullerenol, increased thermoplastic polyurethane dispersibility and gas barrier characteristics. Moreover, Kausar (2016) [25] assessed the thermo-mechanical and fire resistance characteristics of polyurethane/fullerene composite films coated in epoxy. He found that a useful method of producing nonflammable, thermally stable, and mechanically robust materials was to make unique epoxy coated polyurethane/fullerene composite films. Additionally, Kausar (2020) [26] noted the significance of the combination of fullerene and epoxy, which results in a number of positive attributes and excellent performance. The glass transition temperature (T_g) of PU resins can be affected by the fullerene concentration. Fullerenes can reduce polymer chain mobility, resulting in an increase in the T_g. Ristić et al. (2018) [27] reported that increasing the fullerene concentration led to an increase in the T_g, which increased with increasing fullerene content, suggesting enhanced rigidity of the polymer matrix.

Polyurethanes (PUs), rigid or soft, are based on their chemical composition and have a wide range of applications, including buildings, construction, adhesives, coatings, furniture, and medicine [28,29]. PUs are synthesized by the addition of isocyanates to polyols. PUs contains two or more functional groups, such as OH, NH, NH–C═O, and -*O*-, on the basis of two monomers, isocyanates, and polyols. There are different types of factors that affect the chemical structure of PUs and provide new materials with good physico-mechanical properties, and outstanding chemical and water resistance. These factors include the type of isocyanates, polyols, NCO/OH ratio, temperature, solvent, and other additives [30–32]. The chemical structure of PUs can improve their dispersion in conventional solvents, fillers, pigments and plasticizers. PUs have the potential to form complexes with different kinds of pigments and fillers to increase the stiffness of the coating on the surface of the substrates. Coatings based on PUs exhibit high performance and are widely used for concrete, wood, and metals.

In this study, the effect of the fullerene content on the properties of different PUs was investigated. Factors affecting the rheological and thermal properties of the prepared polyurethane/Fullerene composites were studied using different isocyanates and polyols.

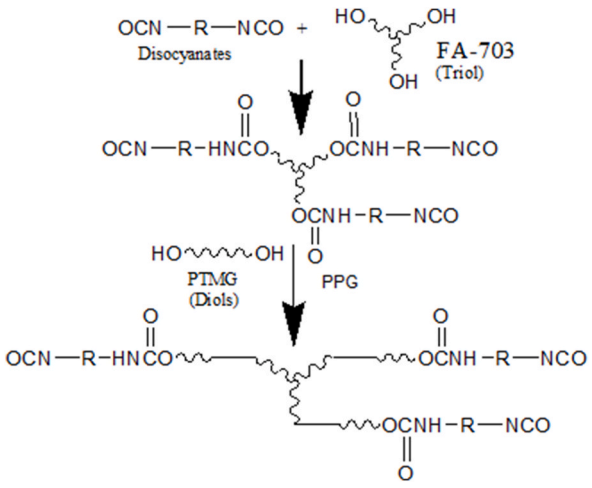

Scheme 1. Formation of PU polymers. R= IPDI, MDI, and HDI.

2. Materials and methods

2.1. Materials

Poly(oxytetramethylene) glycol (PTMG, Mw = 2000 g/mol, Korea PTG, Korea), triol trade name (FA-703, Mw = 3200 g/mol, Korea Polyols, Korea), and polypropylene glycol (PPG, Mw = 4000 g/mol and Mw = 6000 g/mol) were dried and degassed at 80 °C, and 1–2 mm Hg for 2 h before use. Isophorone diisocyanate (IPDI, Mw = 222.29 g/mol, Bayer), methylene diphenyl diisocyanate (MDI, Mw = 250.25 g/mol, Sigma), and hexamethylene diisocyanate (HDI, Mw = 168.2 g/mol, Bayer), were used as received.

2.2. Methods

2.2.1. Preparation of PU polymers

The polyurethane resins were prepared as previously described in the literature [33]. Polymerization was performed in a 500 mL round-bottom, four-necked separable flask with a mechanical stirrer, thermometer, and condenser and a drying tube. The reaction was carried out in a N_2 atmosphere in a constant-temperature oil bath. IPDI, MDI, HDI, and polyols (PTMG and FA703) were charged into the reactor under continuous stirring, and the mixture was heated at 100 °C for 1 h. After that, PPG was added to the mixture and the reaction proceeded at the same temperature until the theoretical NCO value was reached, as determined by the di-*n*-butylamine titration method. The preparation of the prepolymer is shown in Scheme 1. The prepolymers prepared by using different types of isocyanates (IPDI, MDI, and HDI) are shown in Table 1.

2.2.2. Synthesis of fullerene

The synthesis of fullerene C_{60} and C_{70} was carried out in the plasma of an electric arc discharge [12]. In the experiment, graphite rods were used as a carbon source. The synthesis process consists of two stages. In the first stage, the graphite electrodes are annealed by resistive heating with continuous pumping of air from the chamber to a vacuum value of 10^{-3} Torr. In this case, the temperature of the heated electrode can reach 10,000 K due to the high electrical current of 180 A that passes through the graphite electrodes. During annealing, the residual gases, water vapor, and hydrocarbons are desorbed from the pores of the graphite electrodes. In this case, water evaporation occurs at 433.15 K, oxygen-containing groups decompose at 473.15 K, and residual impurities are removed at higher temperatures. In the second stage, after the resistive heating of the electrodes, high-purity helium gas is injected into the chamber up to a pressure of 200 Torr. Furthermore, the electrodes are disconnected and moved to a distance of 1–2 mm from each other, while the values of the direct current and voltage reach 90–200 A and 60–80 V, respectively. After the formation of an electric arc, the voltage stabilizes at 20–30 V due to the constant electrode distance. Thus, carbon vapor is obtained, which is converted into fullerene soot during synthesis. The resulting carbon black dissolves in benzene or toluene. The solution was left for several hours. Then the extract was separated from the insoluble component by filtration. The resulting soluble mixture was evaporated at a temperature of 413.15 K.

2.2.3. Preparation of PU/fullerene composites

The solutions were prepared according to the following procedure: 5 mL of polyurethane was added to 0.003 mg of fullerene and 10 mL of toluene; the concentration was chosen according to the literature sources [34]. To ensure the reproducibility of the results, the preparations were performed three times, and the results obtained were averaged, with all the results being close to one another.

2.3. Characterization

The morphology of the obtained fullerene (fullerite or crystals) was studied by SEM on a Quanta 200i 3D complex. The structural

Table 1
Feed compositions of PUs synthesized with various contents of polyol and isocyanate.

Samples	PU1		PU2		PU3		PU4	
Polyols, OH								
	Wt (g)	Wt (%)	Wt (g)	Wt (%)	Wt (g)	Wt (%)	Wt (g)	Wt (%)
PTMG	148.5	77.49	148.5	77.49	148.5	77.49	148.5	77.49
FA-703	13.4	6.99	13.4	6.99	13.4	6.99	13.4	6.99
PPG 4000	12.5	6.52	12.5	6.52	12.5	6.52	6.25	3.2
PPG 6000							9.375	4.8
Moles of OH (gm/mole)	0.0815		0.0815		0.0815		0.0815	
Isocyanates, OCN								
IPDI-1	17.15	8.9						
MDI			19.38	10				
HDI					13.02	6.9		
IPDI-2							17.15	8.9
Moles of NCO (gm/mole)	0.077		0.077		0.077		0.077	
NCO/OH Molar ratio	0.94		0.94		0.94		0.94	

properties of fullerene were studied by Raman spectroscopy using a solver spectrum spectrometer (NT-MDT) in 180° reflection mode. The excitation source was a laser with a wavelength of $\lambda = 473$ nm. The diameter of the laser spot on the sample was ~2 μm. Optical images of the fullerite were obtained using an optical microscope (Leica DM6000 B, Leica Microsystems). The chemical structure and main functional groups of the prepared polyurethane resins with and without fullerene were investigated using FTIR spectroscopy (MODEL BRUKER, Alpha II). The FTIR spectra were recorded on a Bruker Tensor 37 FTIR spectrometer in the wavenumber range of 4000–400 cm^{-1}. The thermal stability of the prepared polyurethane resins was assessed by TGA/DTA thermal analysis. Measurements were performed between 30 and 900 °C with a 10 °C/min heating rate under a nitrogen atmosphere on a PerkinElmer Simultaneous Analyzer STA 6000. The rheological properties of the prepared polyurethane resins were measured using a Bohlin rheometer, (model CS10, UK). The samples were analyzed using two measuring systems, namely, a Cup Stainless (25 mm) and Cone Plate (CP4 40 mm), according to the viscosity of the latex. The instrument was provided by PC software, through which the measurement conditions were first adjusted, and the resulting data were automatically obtained as a table, graph, and/or absolute value. The conditions for the viscosity measurements were adjusted as follows: initial shear (0.0 s^{-1}), final shear (100 s^{-1}), range (linear), delay (10 s), integration (10 s), proportionality (constant), ramp diring (up), and temperature (isothermal at 25 °C) modes.

3. Results and discussion

Fig. 1 shows the SEM image of the fullerite obtained at a constant current of 180 A. The morphology of the prepared fullerene crystals is similar to that published in the literature [35–37]. Most of the fullerene crystals obtained have a rod shape with a length of several micrometers and a width of hundreds of nanometers (a: Horizontal field width (HFW): 9.95 μm; b: HFW: 2.98 μm; c: HFW: 14.9 μm; d: HFW: 2.98 μm). Some crystals are flower-shaped and grow from one base, and their dimensions are also several micrometers.

Fullerite particles may arrange themselves into precise forms via intermolecular interactions. Rod-shaped structures may be desirable form for reducing surface energy or enhancing packing efficiency. The chemical composition of the resin can affect the assembly of fullerite particles. If the resin has certain functional groups that interact with fullerite, it may enhance its alignment or aggregation into rod-shaped. Structures. SEM analysis was done only for pure fullerene, and SEM analysis was not performed, since the resin is viscous for such analysis. The shots of the rod are characteristic of C_{70}, and the shape of the flowers is characteristic of C_{60}.

Furthermore, the SEM images of fullerenes C_{60} and C_{70} displayed a homogenous size distribution, indicating that C_{60} and C_{70} readily agglomerated due to strong van der Waals forces and extensive π-π stacking interactions [38]. Maintaining controlled processing conditions, such as temperature and mixing speed, is essential for achieving uniform dispersion. Careful monitoring of these parameters during the blending process can help prevent the formation of agglomerates and ensure a homogeneous distribution of

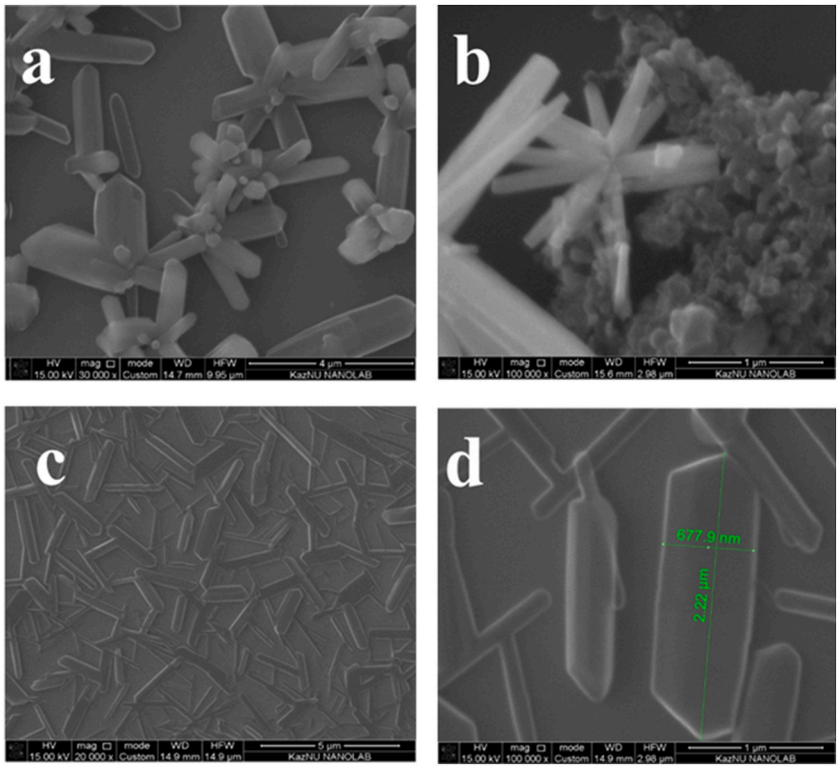

Fig. 1. SEM image of fullerite, mixture of fullerenes C_{60} and C_{70}. a: Horizontal field width (HFW): 9.95 μm; b: HFW: 2.98 μm; c: HFW: 14.9 μm; d: HFW: 2.98 μm.

fullerenes. A homogeneous dispersion of fullerenes was achieved in the present study by stirring for 48 h at 600 °C. Researchers can ensure the homogeneous distribution of fullerenes inside the polyurethane matrix by carefully selecting and improving these procedures, resulting in better composite characteristics and performance.

The emerging field of nanotechnology emphasizes material purity over traditional bulk-scale chemistry. Fullerenes, generated by heating graphite under helium, result in a mixture of C_{60}, C_{70} and large fullerenes. Raman spectroscopy provides a method whereby one can rapidly determine the composition of a mixed fullerene sample in a precise way [39]. Furthermore, a relatively significant resonance enhancement, spectral simplicity (at least for high-symmetry fullerene species), and accessibility all contribute to a robust Raman response [40].

Raman analysis of the fullerene crystals revealed the typical spectrum of fullerene C_{60} and C_{70} (Fig. 2 c). While Fig. 2 (a & b) shows the C_{60} and C_{70}, respectively. This spectrum was obtained upon excitation by a laser at a wavelength of 473 nm. ND filter was used to prevent the destruction of the structure of the studied material and to reduce the laser intensity to a power value of 0.35 mW (1 % of the initial value) (a power value of 0.35 mW- is the optimal parameter for measuring the fullerene crystal lattice; if more power is chosen, then the fullerene will burn). Analysis of the most intense peaks showed that the sample is a combined crystal consisting of fullerenes C_{60} and C_{70}, with a predominance of C_{70}. The peaks at 271, 493, 770, and 1463 cm^{-1} correspond to the characteristic Raman vibrational modes of the C_{60} molecule. The set of peaks at 700, 1065, 1179, 1225, and 1440 cm^{-1} are attributed to C_{70} fullerene [39].

The FTIR spectra of the PU resins prepared with different isocyanate monomers are shown in Fig. 3. As shown in Fig. 3, the characteristic absorption band for the NCO stretching of isocyanate monomers appeared at approximately 2269 cm^{-1}. In addition, the transmittance percentage (peak intensity) for the pure isocyanate monomers was (95 % for NCO), while for the polymers (poly IPDI, poly MDI, and poly HDI), the transmittance percentage decreased to 30 % for poly IPDI, 22 % for poly MDI, 18 % for poly HDI, and 5 % for IPDI polymerized with PPG 6000. The reduction in peak intensity could be attributed to the consumption of the NCO groups during the reaction with the OH groups of the polyols.

In Fig. 3 (a) sample PU1, IPDI-1 without C_{60} (black line) reveals the typical peaks of IPDI-1, a polyurethane produced from isophorone diisocyanate. Peaks are found at 3300 cm^{-1} (N–H stretch), 2900 cm^{-1} (C–H stretch), and 1700-1600 cm^{-1} (C═O stretch). Similar peaks were observed for with C_{60} (red line), however, there was considerable variation in peak intensities and positions, indicating an interaction between C_{60} and the polyurethane matrix. The addition of C_{60} may produce shifts in the peaks due to changes in the polymer network or novel interactions between C_{60} and the polymer chains.

In Fig. 3 (b) sample PU2, MDI without C_{60} (black line) exhibits the typical peaks of methylene diphenyl diisocyanate MDI), which is frequently used in polyurethane manufacturing. Peaks were detected at 3300 cm^{-1} (N–H stretch), and 2900 cm^{-1} (C–H stretch), and significant peaks were detected at 1700-1600 cm^{-1} (C═O stretch). Peaks were still evident for C_{60} (red line), but with different intensities and small shifts, indicating that C_{60} interacts with MDI-based polyurethane. The peak positions and intensities may suggest changes in molecular interactions and structural alterations caused by C_{60} incorporation.

In Fig. 3 (c) sample PU3, HDI without C_{60} (black line) reveals distinctive peaks of HDI (hexamethylene diisocyanate), another component of polyurethanes. Peaks were observed at 3300 cm^{-1} (N–H stretch), 2900 cm^{-1} (C–H stretch), and 1700-1600 cm^{-1} (C═O stretch). The presence of C_{60} (red line) resulted in distinct peak intensities and potential changes in wavenumbers, suggesting its impact

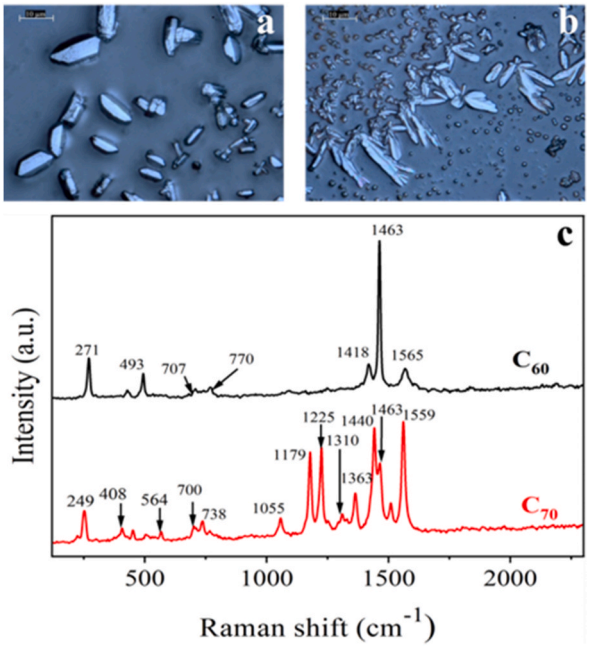

Fig. 2. Optical image (a: C_{60}, b: C_{70}) and Raman spectra of the obtained fullerenes (c).

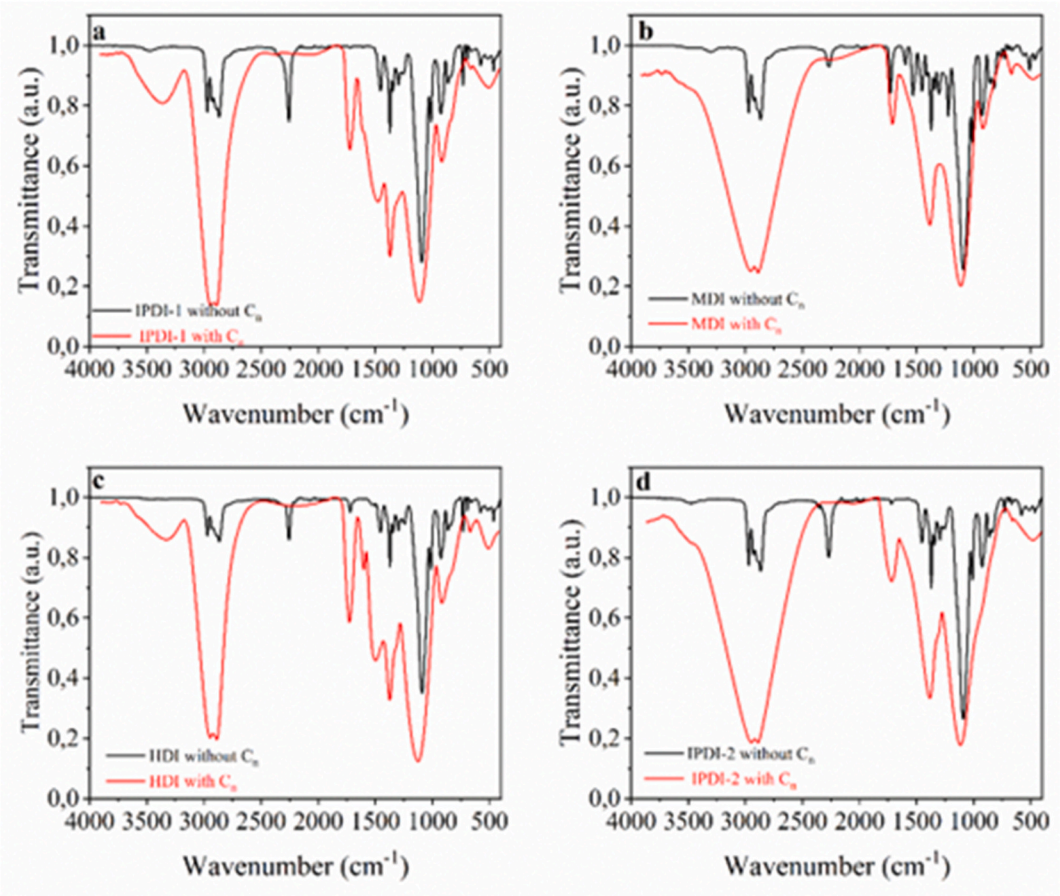

Fig. 3. FTIR spectra of the prepared polyurethanes a) PU1, b) PU2, c) PU3, and d) PU4 with and without fullerene.

on the polymer structure. The incorporation of C_{60} most likely changes the polymer's molecular arrangement and HDI chain interactions.

In Fig. 3 (d) sample PU4, IPDI-2 without C_{60} (black line) is identical to IPDI-1 and shows typical peaks of IPDI-based polyurethane. Peaks at 3300 cm^{-1} (N–H stretch), 2900 cm^{-1} (C–H stretch), and 1700-1600 cm^{-1} (C═O stretch) were detected. C_{60} (red line) interacts with the polyurethane matrix, resulting in variations in peak intensities and shifts in wavenumbers. The addition of C_{60} changes the polymer structure, as shown by the changes in the FTIR spectra.

When C_{60} was present, the FTIR spectra of the samples with C_{60} (red lines) were noticeably from those of the samples without C_{60} (black lines). This suggests a possible physical or chemical interaction between C_{60} and the polyurethane matrix, which modifies the polymer network. Variations in peak intensities and positions point to changes in the structure and molecular interactions of the polymer. The polymer chain mobility, crosslinking density, and general network topology may all be impacted by the addition of C_{60} to the polymer matrix.

For rheological properties, the viscosity of polyurethane resins (PUs) prepared from IPDI, MDI, and HDI isocyanates with polyols (PTMG 200, FA-703, and PPG 4000) and the viscosity of PUs mixed with fullerene were measured (Fig. 4) (a: PU1, b: PU2, c: PU3, and d: PU4) to investigate the effect of fullerene on the rheological properties of the prepared PUs. Fig. 4 shows effect of shear rate (D) on the shear stress and viscosity of the prepared PUs and PUs mixed with fullerene. Generally, viscosity depends on the type of isocyanate, polyol, NCO/OH ratio, and solvent.

To determine the flow characteristics of the obtained PUs and PUs mixed with fullerene, the viscosity of their solutions prepared at a fixed concentration (10 wt%) was measured at different shear rates (0–100 S^{-1}). As shown in the flow curves (Fig. 4), the shear stress increased with increasing shear rate from 0 to 100 S^{-1}. In addition, the shear rate and shear stress of the PUs depend on the isocyanate type. The viscosity of the solutions can be arranged in descending order according to the type of isocyanate, as follows: PU2 > PU4 > PU1 > PU3.

The effect of the shear rate on the shear stress of PUs mixed with fullerene is shown in Fig. 4. The shear stress increased with increasing shear rate of the PUs-fullerene. Additionally, the shear stress is the highest in the case of 3-fullerene and the lowest in the case of 2-fullerene at the same shear rate. However, the shear stress of PUs is greater than that of PUs-fullerene. The flow curves are convex to the shear stress axis and represent the state of increasing shear rate because PUs and PUs-fullerene behave as non-Newtonian

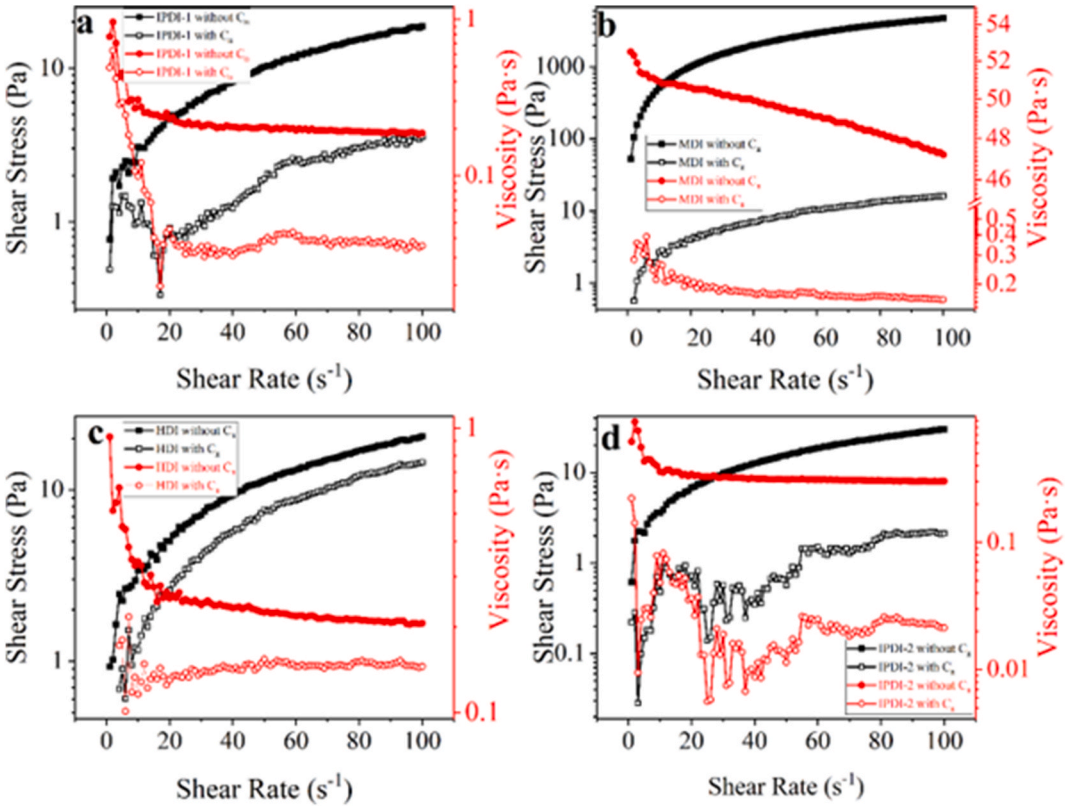

Fig. 4. Rheological properties of the prepared polyurethane resins (PUs) using different isocyanates and PUs mixed with fullerene. a) PU1, b) PU2, c) PU3, and d) PU4.

shear-thinning fluids. The convexity of the flow curves to the shear stress axis implies that the PUs and PUs-fullerene composites have non-Newtonian shear-thinning behavior. This occurs as a result of polymer chain alignment and disentanglement, as well as extra interactions with fullerene particles in composites. This behavior is useful in a wide range of practical applications that require regulated flow and application qualities.

A rheological analysis of a substance exhibiting a non-Newtonian signature suggested that its viscosity is not constant and varies depending on the applied shear rate or stress. Newtonian fluids, on the other hand, behave differently, having a constant viscosity independent of the shear rate. The non-Newtonian property of the polymer matrix is typically considered implicitly in an interaction parameter during the modeling of polymer composite processing. This parameter also includes a number of additional impacts, such as contact and hydrodynamic interactions. However, several experimental investigations have shown that the behavior of fibers in a non-Newtonian fluid differs significantly from that in a Newtonian fluid. Specifically, the fiber orientation kinetics result from the viscoelasticity of the polymer matrix, which differs from that of Jeffrey's solution for a Newtonian matrix [41,42].

Additionally, the viscosity of PU and PU-fullerene was characterized by the formation of a straight line parallel to the shear rate axis, which indicates the Newtonian behavior of the PU and PU-fullerene solutions.

On the other hand, it is also evident that the apparent viscosity of the measured samples slightly decreased with increasing shear rate from 0 to 100 S^{-1} for both PUs and PUs-fullerene. However, the viscosity of 4 is the highest and the viscosity of 3 is the lowest for PU, while the viscosity of PU is higher than that of PU-fullerene. The viscosity of the 1+ solution is the highest and that of the 2+ solution is the lowest. This could be due to the formation of three-dimensional network structures upon mixing PUs with fullerene.

The addition of fullerenes, as nanoparticles, to polyurethane resin leads to a change in the interaction between polymer molecules and fullerenes. These changes affect the rheological properties of the material. Fig. 4 shows that in all cases, the introduction of fullerenes into polyurethane led to a significant decrease in viscosity. This is due to a decrease in the coefficient of friction. It is assumed that fullerene molecules, which are spherical carbon structures, act as molecular bearings, which improve the sliding of polymer molecules relative to each other under the influence of mechanical forces. The addition of fullerenes also changes the shear stress of the polymer mixture, which affects its ability to resist deformation when mechanical stress is applied. The diagrams in Fig. 4 show a decrease in the shear stress of all the samples, which indicates an improvement in the deformation properties of the material. It is important to note that in diagram (d) in Fig. 4, there is a significant change in the behavior of the polyurethane resin when fullerene is added. Unlike the sample without fullerene, which exhibits non-Newtonian behavior, the mixture with the addition of fullerene exhibits Newtonian behavior. However, in other cases, both with and without the addition of fullerene, the polyurethane solutions remain non-Newtonian and exhibit pseudoplastic behavior, despite the decrease in viscosity and shear stress upon the addition of

fullerene. This may indicate a more efficient interaction between polyurethane and fullerene molecules when using the IPDI-2 method. Reducing viscosity and shear stress facilitates the molding and processing of polyurethane resin. In general, the addition of fullerenes to polyurethane resin improves its rheological properties, which makes the material more suitable for various technical and engineering applications.

3.1. Thermal properties of PUs without and with fullerene

TGA is a technique and method for studying the thermal stability of polymers [43]. The thermal behavior of PUs based on different types of isocyanates (aromatic and aliphatic) was evaluated with TGA, and DTG in air at a heating rate of 10 °C/min, and DSC at the same heating rate under a nitrogen atmosphere. TGA thermograms of the PUs are shown in Fig. 5 (a: PU1 with C_n and without C_n, b: PU2 with C_n and without C_n, c: PU3 with C_n and without C_n and d: PU4 with C_n and without C_n. Table 2 summarizes the TGA results of the PUs prepared with different types of isocyanates.

The thermal behavior of the PUs proceeded in two stages for IPDA, MDI, and HDI. Generally, intermolecular hydrogen bonds and the type of isocyanates affect the process of PUs formation, which is related to water loss and cross-linking. The first weight loss was 10 % at 29.49–340.18 °C for IPDI, 8 % at 29.70–380.15 °C for MDI, 5 % at 29.8–360.7 °C for HDI, and 12 % at 29.70–370.6 °C for IPDI. This weight loss can be attributed to the evaporation of residual moisture and solvents. The second weight loss was 84 % for IPDI, 90 % for MDI, 93.5 % for HDI, and 88 % for IPDI at 400 °C. This weight loss could be attributed to the exothermic decomposition of the CO, NCO, and ether groups, which corresponds to the hydrogen bonds due to broken inter- and intramolecular hydrogen bonds. Many factors affect the degradation of polymers, including atmosphere, temperature, type, and composition of the polymer [39]. The maximum polymer degradation temperature (PDT_{max}) of the prepared PUs, corresponding to the maximum rate of weight loss [35,36, 39,43] was measured and is shown in Table 2. All PUs decomposed at 420 °C, which is above the highest rheological measurements employed in this study (Table 2).

On the other hand, Fig. 5 reflects the change in the thermal behavior of PUs due to mixing with fullerene and making a difference or modification of their composition. From the TGA curve, a shift in the first weight loss to 29.28 % for IPDA, 30.21 % for MDI, 20.28 % for HDI, and 33.83 % for IPDI at 29.8–300 °C, as well as a second weight loss was 70.54 % for IPDI, 67.66 % for MDI, 78.35 % for HDI and 65.79 % for IPDI at 420 °C, were observed as the composition varied because of fullerene. However, no change in the PDT_{max} was observed, but it was observed at two *Tonset* temperatures for PUA mixed with fullerene due to the immiscibility of PUs with fluorine as shown in Fig. 5.

Future studies should explore the electrical and optical properties of polyurethane-fullerene composites, particularly for use in

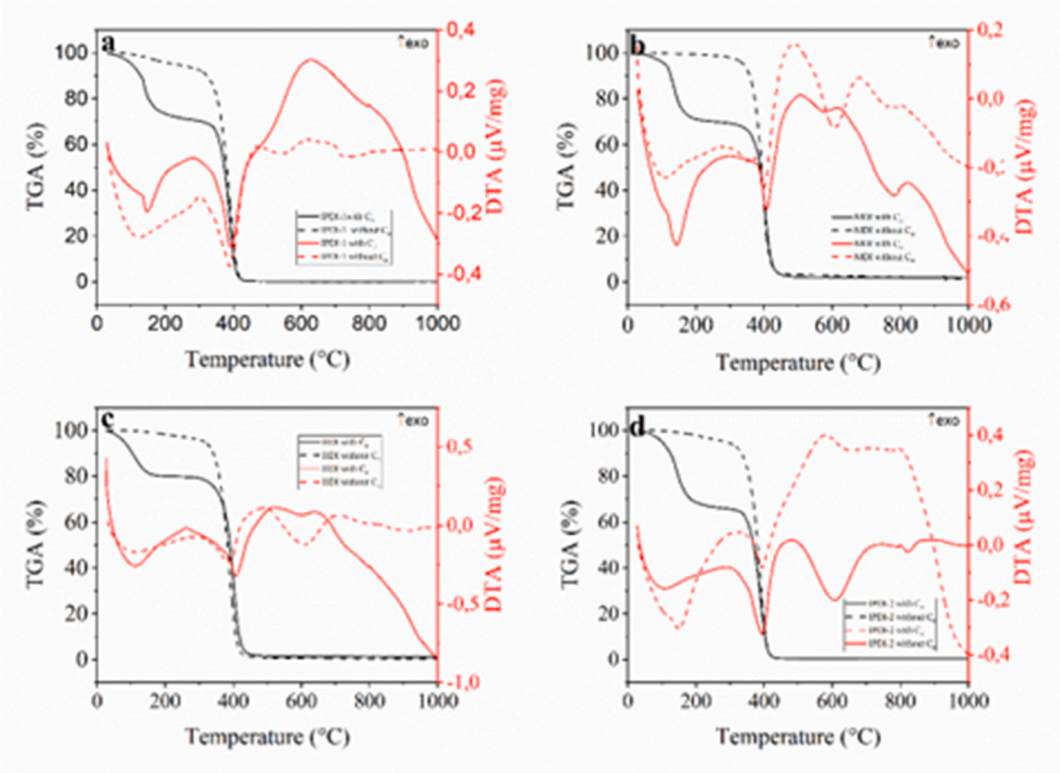

Fig. 5. TGA curves for PUs. a) PU1 with C_n and without C_n, b) PU2 with C_n and without C_n, c) PU3 with C_n and without C_n and d) PU4 with C_n and without C_n.

Table 2
The thermal properties of PU resins without and with fullerene are determined using different isocyanates.

PUs without and with Cn	Decomposition temperatures (°C)	Weight loss (%)	PDT_{max} (°C[b])	T_{onset} (°C)
Isocyanate type				
PU1 without C_n	29.49–340.18	10	420	323.8
	400	84		
PU1 with C_n	29.49–300	29.28	420	135.9
	420	70.54		
PU2 without C_n	29.70–380.15	8	420	380.8
	400	90		
PU2 with C_n	29.70–300	30.21	420	119.1
	420	67.66		
PU3 without C_n	29.70–300	20.8	420	350.4
	400	93.5		
PU3 with C_n	29.70–300	20.8	420	351.1
	420	78.35		
PU4 without C_n	29.70–370.6	12	420	352.9
	400	80		
PU4 with C_n	29.70–300	33.83	420	133.9
	420	79		

sensors, actuators, and optoelectronic devices. They should also explore their environmental and biomedical applications, compatibility with biological systems, and scalability.

Additionally, this study investigated the effect of fullerene content on the properties of polyurethane resin, revealing that it improves rheological properties, processability, and thermal stability, and creates new opportunities for high-temperature materials in automotive, electronics, sensors, and optoelectronics, resulting in advanced formulations with improved performance across a variety of industries.

4. Conclusion

Polyaddition polymerization was used successfully to synthesize polyurethane resins (PUs). The intensity of the NCO signal decreased from 95 % to 15–30 % in the FTIR spectra due to its consumption by the polyols (OH). The thermal and rheological properties of the PU resins with or without fullerene were examined. The findings revealed that the characteristics of PU resins are affected by the type of isocyanate monomer, polyol, and fullerene used. However, compared to aromatic isocyanates, PUs containing fullerene improved the rheological and thermal properties of aliphatic isocyanates.

Ethics approval

Not applicable.

Consent

All the authors agreed with the content, gave explicit consent to submit the study, and obtained consent from the responsible authorities at the institute/organization where the work was carried out.

Availability of data

The data will be made available upon request.

Material and/or code availability

Not applicable.

Funding sources

Scientific Research Program from the Committee of Science of the Ministry of Science and Higher Education of the Republic of Kazakhstan (grant number: BR18574080).

CRediT authorship contribution statement

Nazym Ye Akhanova: Writing – original draft. **El-Sayed Negim:** Writing – review & editing, Conceptualization. **Yerassyl**

Yerlanuly: Data curation, Conceptualization. **Didar G. Batryshev:** Resources, Methodology. **Mohamed M. Eissa:** Resources, Investigation. **Dmitry Yu Schur:** Investigation, Data curation. **Tlekkabul S. Ramazanov:** Methodology, Investigation, Data curation. **Khaldun M. Al Azzam:** Writing – review & editing. **Mukhit M. Muratov:** Validation, Supervision. **Maratbek T. Gabdullin:** Validation, Methodology, Formal analysis.

Declaration of competing interest

The authors declare no potential conflicts of interest.

Acknowledgments

The authors thank the Scientific Research Program (grant number: BR18574080) from the Committee of Science of the Ministry of Science and Higher Education of the Republic of Kazakhstan.

References

[1] P.J. F Harris, Fullerene Polymers: A Brief Review. C 6 (4) (2018) 71, https://doi.org/10.3390/c6040071.
[2] R. Mishra, J. Militky, Carbon-based nanomaterials. Nanotechnology in Textiles, 2019, pp. 163–179, https://doi.org/10.1016/b978-0-08-102609-0.00003-1.
[3] G.L.C. Moura, A.M. Simas, Two-Photon absorption by fluorene derivatives: systematic molecular design, J. Phys. Chem. C 114 (13) (2010) 6106–6116, https://doi.org/10.1021/jp100314c.
[4] I.V. Kurdyukova, A.A. Ishchenko, Organic dyes based on fluorene and its derivatives, Russ. Chem. Rev. 81 (3) (2012) 258–290, https://doi.org/10.1070/rc2012v081n03abeh004211.
[5] S. E, K. Negim, Omurbekova, L. Bekbayeva, A. Abdelhafiz, Effect of NCO/OH ratio on the physico-mechanical properties of polyurethane-polyurea hybrid spray coatings. Egypt, J. Chem. 63 (11) (2020) 4519–4524, https://doi.org/10.21608/ejchem.2020.23845.2416.
[6] K. Ogawa, Two-Photon absorbing molecules as potential materials for 3D optical memory, Appl. Sci. 4 (1) (2014) 1–18, https://doi.org/10.3390/app4010001.
[7] L. Persze, L. Tolvaj, Photodegradation of wood at elevated temperature: colour change, J. Photochem. Photobiol. B Biol. 108 (2012) 44–47, https://doi.org/10.1016/j.jphotobiol.2011.12.008.
[8] C. Chen, Y. Hsu, H. Chou, K.R.J. Thomas, J.T. Lin, C. Hsu, Dipolar compounds containing fluorene and a heteroaromatic ring as the conjugating bridge for high-performance dye-sensitized solar cells, Chem. Eur J. 16 (10) (2010) 3184–3193, https://doi.org/10.1002/chem.200903151.
[9] K. Lim, C. Kim, J. Song, T. Yu, W. Lim, K. Song, P. Wang, N. Zu, J. Ko, Enhancing the performance of organic dye-sensitized solar cells via a slight structure modification, J. Phys. Chem. C 115 (45) (2011) 22640–22646, https://doi.org/10.1021/jp2070776.
[10] A.W. Woodward, A. Frazer, A.R. Morales, J. Yu, A.F. MooreAD, A.D. Campiglia, E.V.V. Jucov, T. Timofeeva, K.D. Belfield, Two-photon sensitized visible and near-IR luminescence of lanthanide complexes using a fluorene-based donor–π-acceptor diketonate, Dalton Trans. 43 (44) (2014) 16626–16639, https://doi.org/10.1039/c4dt01507j.
[11] E.S.M. Negim, T. Ketegenov, G.S. Irmukhametova, I.N. Sultanbekova, T.N. Tastambekova, G.A. Mun, The effect of TDI, PTMG and DMPA on the physico-mechanical properties of polyurethane dispersion containing aromatic isocyanate, Int. J. Biol. Chem. 9 (1) (2016) 68–72, https://doi.org/10.26577/2218-7979-2016-9-1-68-72.
[12] M. Paukov, C. Kramberger, I. Begichev, M. Kharlamova, M. Burdanova, Functionalized fullerenes and their applications in electrochemistry, solar cells, and nanoelectronics, Materials 16 (3) (2023) 1276, https://doi.org/10.3390/ma16031276.
[13] S.W. Ko, H. Chung, Preparation of C60 fullerene nanowhisker–CuS nanoparticle composites and photocatalyst for rhodamine B degradation under blue light emitting diode irradiation, Eurasian Chem-Technol J. 25 (2) (2023) 65, https://doi.org/10.18321/ectj1496.
[14] R. Zhang, L. Guo, I.B. Obot, Anti-Corrosive Nanomaterials, CRC Press, 2023, https://doi.org/10.1201/9781003331124.
[15] A. Khurshid, A. Saeed, Organic–organic Mixed Nanocomposites as Anticorrosive Coatings. Smart Anticorrosive Materials, Elsevier, 2023, pp. 261–303, https://doi.org/10.1016/b978-0-323-95158-6.00001-1.
[16] A. Kausar, Potential of polymer/fullerene nanocomposites for anticorrosion applications in the biomedical field, J. Compos. Sci. 6 (12) (2022) 394, https://doi.org/10.3390/jcs6120394.
[17] A.E. Tarasov, D.V. Anokhin, Y.V. Propad, E.A. Bersenev, S.V. Razorenov, G.V. Garkushin, E.R. Badamshina, Synergetic effect of fullerene and graphene oxide nanoparticles on mechanical characteristics of cross-linked polyurethanes under static and dynamic loading, J. Compos. Mater. 53 (26–27) (2019) 3797–3805, https://doi.org/10.1177/0021998319848077.
[18] X. Wang, J. Hu, Y. Li, J. Zhang, Y. Ding, The surface properties and corrosion resistance of fluorinated polyurethane coatings, J. Fluor. Chem. 176 (2015) 14–19, https://doi.org/10.1016/j.jfluchem.2015.04.002.
[19] E.l.M. Negim, L. Bekbayeva, G.A. Mun, Y.A. Zhalyrkasyn, M.I. Saleh, Effects of NCO/OH ratios on physico- mechanical properties of polyurethane dispersion, World Appl. Sci. J. 14 (2011) 402–407.
[20] F. Bolze, S. Jenni, A. Sour, V. Heitz, Molecular photosensitisers for two-photon photodynamic therapy, Chem. Commun. 53 (96) (2017) 12857–12877, https://doi.org/10.1039/c7cc06133a.
[21] M. Gangopadhyay, S.K. Mukhopadhyay, S. Gayathri, S. Biswas, S. Barman, S. Dey, D.P. Singh, Fluorene–morpholine-based organic nanoparticles: lysosome-targeted pH-triggered two-photon photodynamic therapy with fluorescence switch on–off, J. Mater. Chem. B 4 (10) (2016) 1862–1868, https://doi.org/10.1039/c5tb02563j.
[22] N. Akhanova, Y. Yerlanuly, D. Batryshev, T. Kulsartov, Y. Chikhray, T. Ramazanov, A. Veziroglu, D. Schur, W. Kang, M. Gabdullin, The study of deuterium permeability of film-forming inhibitors with the addition of fullerenes, Int. J. Hydrog Energy 46 (10) (2021) 7426–7431, https://doi.org/10.1016/j.ijhydene.2020.11.241.
[23] Y. Kanbur, U. Tayfun, Development of multifunctional polyurethane elastomer composites containing fullerene: mechanical, damping, thermal, and flammability behaviors, J. Elastom. Plast. 51 (3) (2018) 262–279, https://doi.org/10.1177/0095244318796616, 2018.
[24] R. Dobashi, K. Matsunaga, M. Tajima, Effects of fullerene derivatives on the gas permeability of thermoplastic polyurethane elastomers, J. Appl. Polym. Sci. 131 (6) (2013), https://doi.org/10.1002/app.39986.
[25] A. Kausar, Estimation of thermo-mechanical and fire resistance profile of epoxy coated polyurethane/fullerene composite films, Fuller. Nanotub. Car. N. 24 (6) (2016) 391–399, https://doi.org/10.1080/1536383x.2016.1172067.
[26] A. Kausar, Fullerene nanofiller reinforced epoxy nanocomposites—developments, progress and challenges, Mater. Res. Innov. 25 (3) (2020) 175–185, https://doi.org/10.1080/14328917.2020.1748794.
[27] I. Ristić, I. Krakovsky, T. Janić, S. Cakić, A. Miletić, M. Jotanović, T. Radusin, The influence of the nanofiller on thermal properties of thermoplastic polyurethane elastomers, J. Therm. Anal. Calorim. 134 (2018) 895–901, https://doi.org/10.1007/s10973-018-7278-8.
[28] F. Yu, L. Cao, Z. Meng, N. Lin, X.Y. Liu, Crosslinked waterborne polyurethane with high waterproof performance, Polym. Chem. 7 (23) (2016) 3913–3922, https://doi.org/10.1039/c6py00350h.
[29] L. Li, X. Wang, Z. Li, W. Bi, Y. Li, Y. Qi, Q. Dong, The synthesis and curing kinetics study of a new fluorinated polyurethane with fluorinated side chains attached to soft blocks, New J. Chem. 40 (1) (2016) 596–605, https://doi.org/10.1039/c5nj01772f.

[30] H. Blattmann, M. Fleischer, M. Bähr, R. Mülhaupt, Isocyanate- and phosgene-free routes to polyfunctional cyclic carbonates and green polyurethanes by fixation of carbon dioxide, Macromol. Rapid Commun. 35 (14) (2014) 1238–1254, https://doi.org/10.1002/marc.201400209.
[31] L. Maisonneuve, O. Lamarzelle, E. Rix, E. Grau, H. Cramail, Isocyanate-Free routes to polyurethanes and poly(hydroxy Urethane)s, Chem. Rev. 115 (22) (2015) 12407–12439, https://doi.org/10.1021/acs.chemrev.5b00355.
[32] J. Li, X. Zhang, Z. Liu, W. Li, J. Dai, Studies on waterborne polyurethanes based on new medium length fluorinated diols, J. Fluor. Chem. 175 (2015) 12–17, https://doi.org/10.1016/j.jfluchem.2015.02.015. BV.
[33] M.M.H. Ayoub, M.M. Ei-Awady, H.E. Nasr, S.M. Negim, Synthesis and rheological properties of some styrene/methacrylate copolymer latices, Polym. Plast. Technol. Eng. 42 (5) (2003) 863–880, https://doi.org/10.1081/ppt-120025000.
[34] L.V. Tsetkova, V.A. Keskinov, N.A. Charykov, N.I. Alekseev, E.G. Gruzinskaya, K.N. Semenov, V.N. Postnov, O.A. Krokhina, Extraction of fullerene mixture from fullerene soot with organic solvents, Russ. J. Gen. Chem. 81 (5) (2011) 920–926, https://doi.org/10.1134/s1070363211050136.
[35] J.A. Rather, A.J. Al Harthi, E.A. Khudaish, A. Qurashi, A. Munam, P. Kannan, An electrochemical sensor based on fullerene nanorods for the detection of paraben, an endocrine disruptor, Anal. Methods 8 (28) (2016) 5690–5700, https://doi.org/10.1039/c6ay01489e.
[36] K. Vimalanathan, R.G. Shrestha, Z. Zhang, J. Zou, T. Nakayama, C.L. Raston, Surfactant-free fabrication of fullerene C_{60} nanotubules under shear, Angew. Chem. Int. Ed. 56 (29) (2016) 8398–8401, https://doi.org/10.1002/anie.201608673.
[37] S. Goodarzi, T. Da Ros, J. Conde, F. Sefat, M. Mozafari, Fullerene: biomedical engineers get to revisit an old friend, Mater. Today 20 (8) (2017) 460–480, https://doi.org/10.1016/j.mattod.2017.03.017.
[38] M. Zhang, X. Wang, Y. Bai, Z. Li, B. Cheng, C_{60} as fine fillers to improve poly(phenylene sulfide) electrical conductivity and mechanical property, Sci. Rep. 7 (4443) (2017) 4443, https://doi.org/10.1038/s41598-017-04491-1.
[39] J.B. Kimbrell, C.M. Crittenden, W.J. Steward, F.A. Khan, A.C. Gaquere-Parker, D.A. Stuart, Analysis of mixtures of C60and C70by Raman spectrometry, Nanosci Methods 3 (1) (2014) 40–46, https://doi.org/10.1080/21642311.2014.976776.
[40] H. Kuzmany, R. Pfeiffer, M. Hulman, C. Kramberger. Raman spectroscopy of fullerenes and fullerene–nanotube composites. A. C. Ferrari & J. Robertson (Eds.), Philosophical Transactions of the Royal Society of London. Series A: Mathematical, Physical and Engineering Sciences (Vol. 362, Issue 1824, pp. 2375–2406). https://doi.org/10.1098/rsta.2004.1446.
[41] N. Ouari, A. Kaci, A. Tahakourt, M. Chaouche, Rheological behaviour of fibre suspensions in non-Newtonian fluids, Appl. Rheol. 21 (2011) 54801, https://doi.org/10.3933/ApplRheol-21-54801.
[42] L. Pu, P. Xu, M. Xu, J. Song, M. He, Effect of fiber on rheological properties and flow behavior of polymer completion fluids, ACS Omega 6 (27) (2021) 17136–17148, https://doi.org/10.1021/acsomega.0c05346, 2021.
[43] K. Syrmanova, E. Negim, J. Kaldybekova, A.M. Tuleuov, Epoxylitane ?ompositions modification with using thermoplastic polyurethane, Orient. J. Chem. 32 (1) (2016), https://doi.org/10.13005/ojc/320101, 01–07.